Preparation and Properties of Transparent and Conducting Nylon 6-Based Composite Films

SUNG SOON IM* and SUNG WEON BYUN

Department of Textile Engineering, College of Engineering, Hanyang University, Seoul, South Korea

SYNOPSIS

Highly transparent and conducting polypyrrole–(PPy–N) and polyaniline–nylon 6 (PA–N) composite films could be easily obtained by immersing nylon 6 films containing pyrrole or aniline into an oxidant solution such as aqueous $FeCl_3$ solution or aqueous $(NH_4)_2S_2O_8$ solution containing HCl. The conductivity, transmittance, and mechanical properties of these composite films were affected by the preparative conditions. The maximum conductivity and transmittance of the PPy–N composite films were 10^{-3} S/cm and about 75% at 550 nm, and in the case of the PA–N composite films, 10^{-2} S/cm and 75%, respectively. The morphology of PPy–N and PA–N composite films depended on the polymerization conditions, which might be due to the difference in the polymerization speed of pyrrole or aniline in polymer matrices. These PPy–N and PA–N composite films exhibited good environmental stability and excellent mechanical properties. © 1994 John Wiley & Sons, Inc.

INTRODUCTION

Recently, there has been the increased industrial demand for transparent and conducting materials in various applications such as electrooptical devices.[1] But, so far, all transparent and conducting films commercially used are inorganic-based thin metallic films, e.g., tin oxide and indium–tin oxide thin films.[2–5] In processing these inorganic thin films, high-vacuum production conditions and heating of the substrates are necessary for sputter-coating.[6] Focus has been put on the development of transparent and conducting polymeric films, because conducting polymers can offer the possibility of simpler and cheaper processes than those of inorganic materials for the preparation of transparent and conducting materials.[7,8] However, little work has been done on these high-tech materials.

In this study, two kinds of transparent and conducting nylon 6-based composite films have been prepared by immersing highly transparent nylon 6 films containing monomer such as pyrrole or aniline into various aqueous oxidant solutions. First, we carefully studied the interaction between polymer matrices and monomers, because low molecular weight liquids are capable of inducing physical modifications in solid polymers, such as reversible swelling, irreversible microfailure, induced crystallization, and even dissolution. By the character of their actions on polymers, liquids can be conditionally divided into two groups: chemically active and physically active. Chemically active liquids affect first of all the covalent bonds and break them down. Physically active liquids affecting mainly the intermolecular interactions can also be conditionally subdivided into two groups: The first group involves liquids causing swelling of a polymer and forming as a result solution with a polymer. The second group involves physically inactive liquids in the absence of external mechanical stresses. The nature of the low molecular weight liquid compound, the solvent, was an important criterion, since polymers are affected by various solvents to different degrees.[9] Therefore, the solubility parameters of polymer matrices and monomers were investigated. Then, the diffusion behaviors of monomers in the polymer matrices and the optimum reaction conditions of these composite films were also studied. Additionally, the effects of the preparative conditions on the conductivity, transmittance, and mechanical properties of these composite films were investigated.

* To whom correspondence should be addressed.

Journal of Applied Polymer Science, Vol. 51, 1221–1229 (1994)
 CCC 0021-8995/94/071221-09

EXPERIMENTAL

Materials and Reagents

Poly(ethylene terephthalate) (PET) film (thickness 30 μm, degree of crystallinity $X_c < 4\%$, Sunkyung Ind.) and biaxially stretched nylon 6 film (thickness 10 μm, degree of crystallinity $X_c = 20.6\%$, Unitika Ltd.) were used as polymeric matrices. The monomers such as pyrrole and aniline were distilled under vacuum before use. All reagents used in this work were special grade and used without further purification.

Preparation of Nylon 6-based Composite Films

Figure 1 is a schematic diagram of the transparent and conducting nylon 6-based composite film preparation process. Before testing, nylon 6 films were washed with water and methanol and heated to 110°C for dry treatment. The dry nylon 6 films were soaked in pure pyrrole or aniline monomer, and the monomer-absorbed nylon 6 films were blotted with filter paper. Then, the pyrrole-absorbed nylon 6 film was immersed in an aqueous $FeCl_3$ solution (used as oxidizing agent) and pyrrole absorbed in nylon 6 film was chemically polymerized by $FeCl_3$. The $FeCl_3$ concentration was varied in the range of 1–3.5 mol % and the ranges of polymerization time and temperature were 5 min to 4 h and −10–60°C, respectively. The aniline-absorbed nylon 6 film was dipped into aqueous $(NH_4)_2S_2O_8$ solution (and HCl as a proton acid) after treatment by the HCl solution. The $(NH_4)_2S_2O_8$ concentration was varied with the range of 0.125–1 mol % and the ranges of polymerization time and temperature were the same as with pyrrole. These composite films were washed well with distilled water and dried *in vacuo* at room temperature for 24 h.

To obtain highly transparent and conducting composite films, the diffusion temperature of the monomers into the polymer matrix, the polymerization time and temperature, and the concentration and acidity of oxidant solutions must be controlled.

Measurements

Sorption properties of pyrrole and aniline in the polymer matrix were measured by the weighing method on the basis of the weight change of the films before and after absorbing the monomers. The conductivity of the composite films was measured

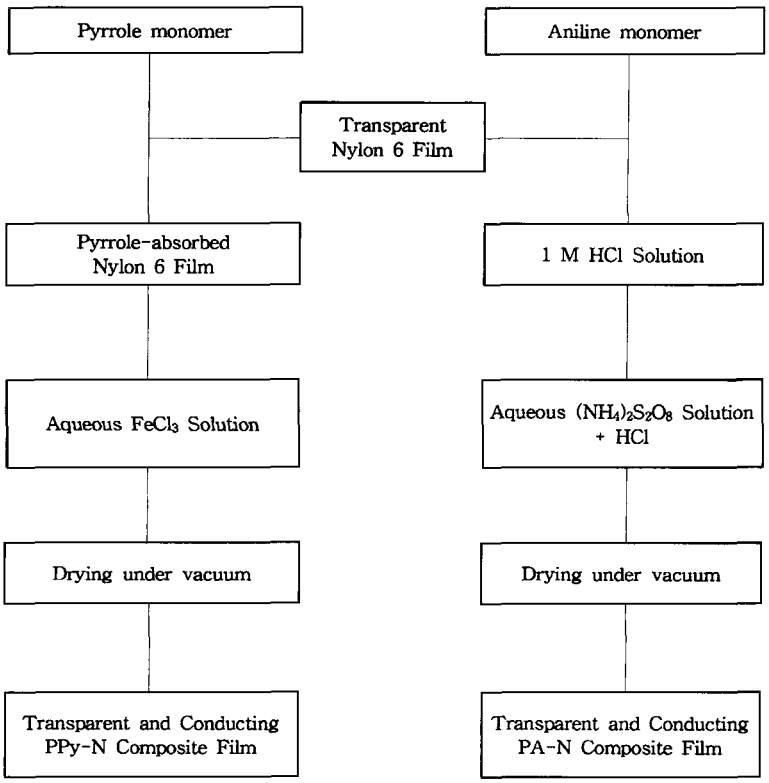

Figure 1 Schematic diagram of nylon 6-based composite film preparation process.

Table I Solubility Parameters Calculated from Cohesive Energy Density

	Nylon 6	PET	Pyrrole	Aniline
Solubility parameter $(cal/cm^3)^{1/2}$				
aliphatic part	13.5	12.1		
aromatic part		9.8	10.5	10.3

by using the standard four-probe method. The transmittance of the composite films was measured with a Shimadzu UV-240 spectrophotometer and pristine nylon 6 film was used as a reference. The morphology of the composite films was investigated with a JEOL JSM-350CF scanning electron microscope and X-ray diffraction patterns were registered using a Rigaku RAD-C employing CuKα radiation. The mechanical properties were tested with a Tensilon/UTM-4-100 at room temperature.

RESULTS AND DISCUSSION

Interaction Between Polymer and Monomers

Table I shows the solubility parameters of matrix polymers and monomers calculated from the cohesive energy density.[10] The difference of the solubility parameters between PET and the monomers is smaller than that between nylon 6 and the monomers, which may mean that a significant interaction can exist between PET and the monomers.

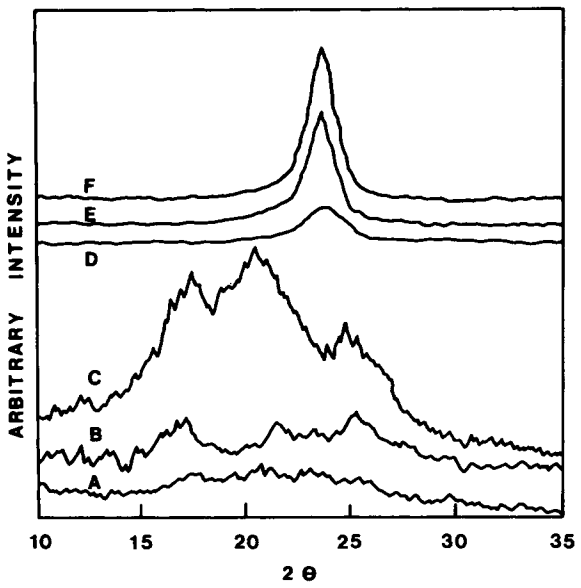

Figure 2 Wide-angle X-ray diffraction patterns of (A) pristine PET, (B) PPy–PET composite film, (C) pyrrole-absorbed PET, (D) PPy–N composite film, (E) pyrrole-absorbed nylon 6 film, and (F) pristine nylon 6 film.

Figure 2 shows the wide-angle X-ray diffraction (WXRD) patterns of PET and nylon 6 films. There is no diffraction peak in pristine PET film [Fig. 2(A)], which means that the PET film can be regarded approximately as an isotropic amorphous film. However, when the PET absorbs pyrrole, three diffraction peaks appear, which can exist in the crystalline polyester at 17.5°, 21.6°, and 26.1° [Fig. 2(C)]. This may indicate that PET has a strong interaction with pyrrole as shown in Table I and that pyrrole can induce the crystallization of PET film. The ability of low molecular weight, interactive penetrants to produce physical modifications such as crystallization in PET is well known and this phenomenon is often called solvent-induced crystallization (SINC).[11] For the results, the pyrrole-absorbed PET film becomes opaque and brittle. But it is found that new diffraction peaks do not appear in pyrrole-absorbed nylon 6 film, nor do any physical changes occur [Fig. 2(E)]. When polypyrrole is polymerized in these polymer matrices, the crystal peak of polymer matrices is decreased [Fig. 2(B) and (D)]. It seems that polypyrrole partially destroys the crystal structure of polymer matrices during the polymerization.

These phenomena also appeared in the case of aniline. Therefore, we selected only nylon 6 film as a polymer matrix in following study.

Diffusion Behaviors of Monomers in the Nylon 6 Film

Figure 3 shows kinetics of mass uptake of pyrrole and aniline in nylon 6 film measured at 20°C, plotted as a function of the square root of the diffusion time. In the case of pyrrole and aniline, the initial portion of the mass uptake curves was approximately linear with the square root of the immersed time, meaning that these are the well-known diffusion-controlled system: the Fickian-type diffusion. For Fickian-type

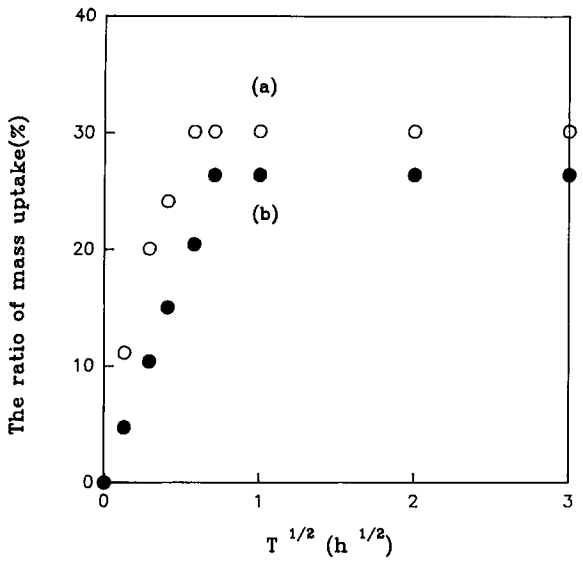

Figure 3 Sorption kinetics of (a) pyrrole and (b) aniline in nylon 6 film at 20°C.

diffusion, the diffusion coefficient, D, can be determined from the initial slope of the mass uptake vs. the square root of diffusion time plot using the following equation[12]:

$$\frac{M_t}{M_\infty} = \frac{4}{l}\sqrt{\frac{D \cdot t}{\pi}} \qquad (1)$$

where M_t and M_∞ are the mass uptake at time t and ∞, and l is the thickness of the film. According to Figure 3, the equilibrium mass uptakes of pyrrole and aniline in nylon 6 film were estimated at about 30 and 26.4%, respectively. From eq. (1), the diffusion coefficients of pyrrole and aniline in nylon 6 film can be calculated to be about 2.01×10^{-14} and 1.06×10^{-14} m^2/s, respectively.

The activation energy of diffusion, E_d, can be determined from the slope of the logarithm plot of the observed diffusion coefficient at different temperatures vs. the reciprocal of the absolute temperature using the following equation[13]:

$$D = D_0 \times \exp(-E_d/RT) \qquad (2)$$

where D_0 is the preexponential factor; R, the gas constant (8.314×10^{-3} kJ/K mol); and T, the temperature in Kelvin. From eq. (2), the diffusion activation energy of pyrrole and aniline in the nylon 6 film can be calculated to be about 4.8 and 5.9 kJ/mol, respectively.

UV-Visible Absorption Spectra of PPy–N and PA–N Composite Films

Figure 4 shows UV-vis absorption spectra of PPy–N composite films for various polymerization times. The transmittances of these composite films at 550 nm gradually decrease from about 75 to 45% with respect to the polymerization times. The new absorption band appears in the range 400–500 nm with increasing polymerization time. It seems that this absorption band is due to π–π^* transition.[14] This absorption band is clearer at 2 h, which corresponds with the conductivity maximum at 2 h. The transmittance of PPy–N composite film under optimum conditions is greater than 70% over the range 500–800 nm.

In the case of PA–N composite films, it was found that the typical absorption spectrum of the emeraldine salt form of polyaniline[15–17] appears and the transmittance is greater than 70% over the range 490–630 nm. Therefore, it was found that the PPy–N and PA–N composite films (thickness 10 μm) were highly transparent in the UV-visible regions.

Effects of the Preparative Conditions on the Conductivity and Transmittance

Figures 5 and 6 show the effects of the oxidant concentration on the conductivity and transmittance of the PPy–N and PA–N composite films, respectively. In Figure 5, the conductivity of the PPy–N composite film increases with $FeCl_3$ concentration and reaches a maximum value at 2.5 M of $FeCl_3$, then tends to decrease. Above 2.5 M $FeCl_3$ concentrations, it seems that a polypyrrole layer that retards the diffusion of the oxidant solution is formed on the surface of nylon 6 film because the polypyrrole is polymerizing too fast, thus generating the nonuniform composite films and decreasing the conductivity of the PPy–N composite film. The transmittance of the PPy–N composite film gradually decreases with $FeCl_3$ concentration and then tends to level off at about 3.0 M of $FeCl_3$. This behavior also was apparent in the case of the PA–N composite films (Fig. 6).

The conductivity and the transmittance of these PPy–N and PA–N composite films were also affected by the polymerization time, temperature, and acidity of oxidant solutions. In forming a highly transparent and conducting PPy–N composite film, the optimum conditions of oxidant concentration, polymerization time, and temperature were found to be 2.5 M of $FeCl_3$, 2 h, and 20°C, respectively. In the case of PA–N composite films, the optimum oxidant con-

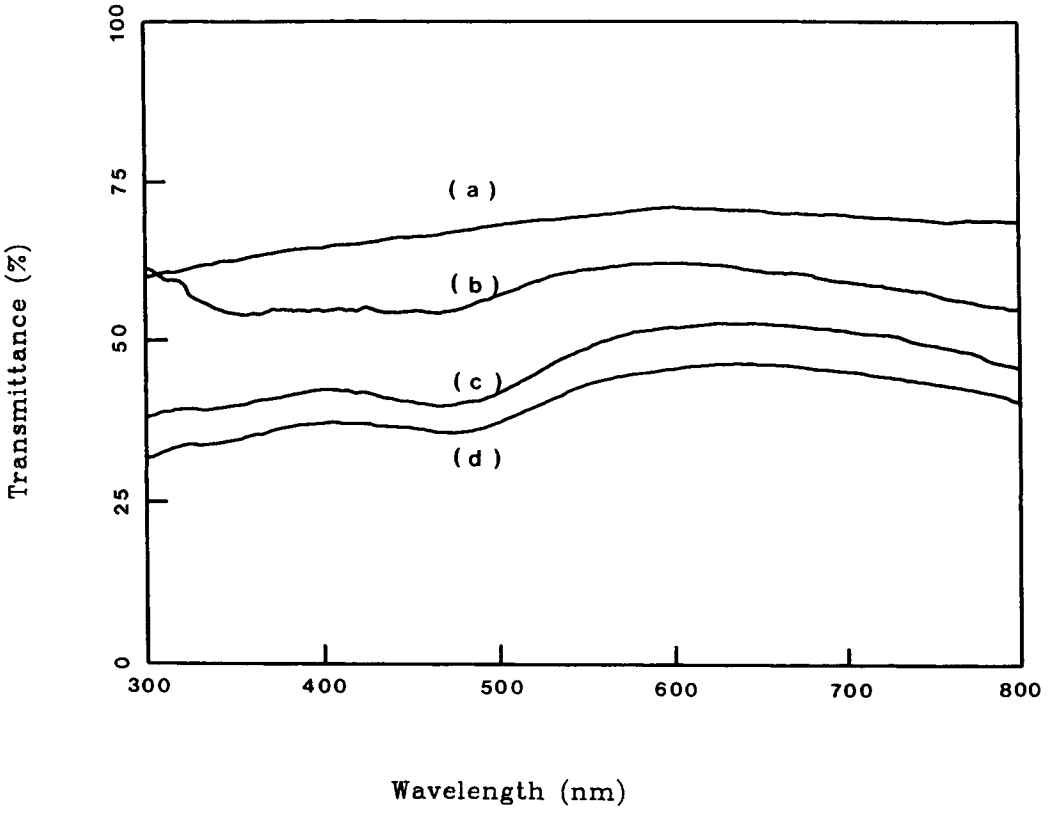

Figure 4 UV-visible spectra of PPy–N composite film with reaction time: (a) 5 min, (b) 30 min, (c) 2 h, (d) 4 h. Diffusion time: 30 min; diffusion temperature: 20°C; $FeCl_3$ concentration: 2.5 *M;* reaction temperature: 20°C.

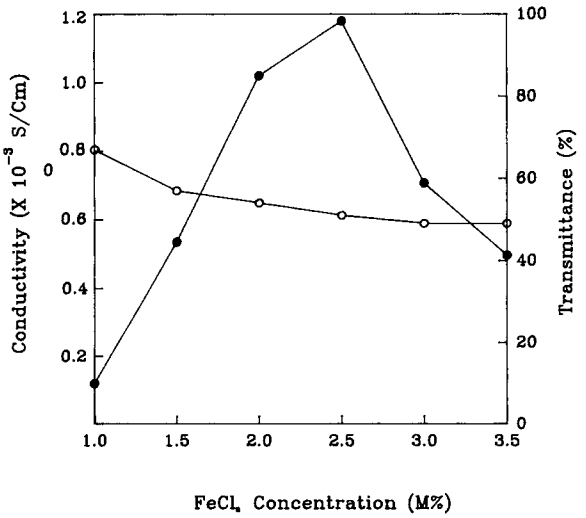

Figure 5 Variation in the (●) conductivity and (○) transmittance with $FeCl_3$ concentration for PPy–N composite film. Diffusion time: 30 min; diffusion temperature: 20°C; reaction time: 2 h; reaction temperature: 20°C.

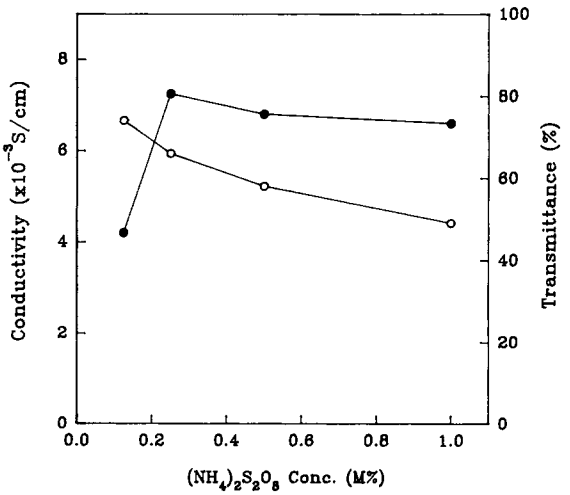

Figure 6 Variation in the (●) conductivity and (○) transmittance with $(NH_4)_2S_2O_8$ concentration for PA–N composite film. Diffusion time: 40 min; diffusion temperature: 20°C; reaction time: 10 min; reaction temperature: 30°C; HCl concentration: 1 *M*.

centration was 0.25 M of $(NH_4)S_2O_8$ under the conditions of a polymerization time of 10 min, reaction temperature of 30°C, and HCl concentration of 2 M.

Morphology of These Composites

Figure 7 shows the scanning electron microscopy (SEM) photographs of the surface for the original nylon 6, pyrrole-absorbed nylon 6, and various PPy–N composite films. The SEM photographs display the flat surface for the original nylon 6 film and the traces by diffusion of pyrrole monomer for the pyrrole-absorbed nylon 6 film. The surface of the PPy–N composite film polymerized at 0°C is coarser than that of PPy–N film polymerized at 20°C. In Figure 7, the conductivity of (d-polymerized at 20°C) is better than that of (c-polymerized at 0°C) and the transmittance of (c) is better than that of (d). Therefore, it is obvious that the polymerization conditions affect the morphology of the composite films, and the surface morphology also greatly affects the conductivity and transmittance of the PPy–N composite films.

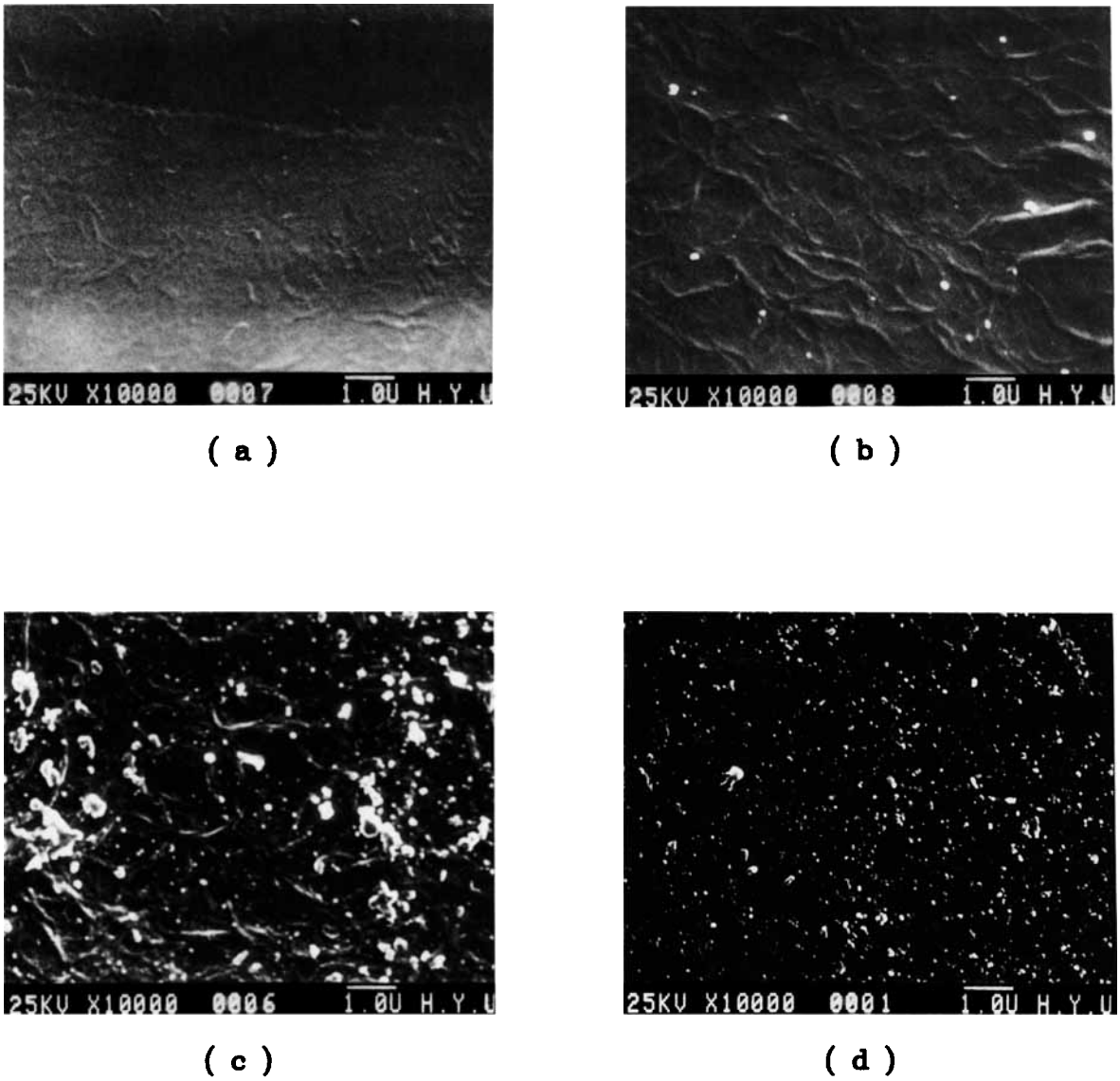

Figure 7 Scanning electron micrographs of PPy–N composite film: (a) prestine nylon 6 film; (b) pyrrole-absorbed nylon 6; (c) PPy–N composite film: polymerization temp. 0°C, $FeCl_3$ concentration 2.5 M, polymerization Time 2 h; (d) PPy–N composite film: polymerization temp. 20°C, $FeCl_3$ concentration 2.5 M, polymerization Time 2 h.

These phenomena also appeared in the case of PA–N composite films (Fig. 8). In the case of PA–N composite film, the surface morphology is the most uniform and dense at 30°C, as seen in Figure 8(c), and the conductivity is also at a maximum. From these results, it was found that the conductivity and transmittance were affected by the surface structure of the composite film.

Electrical Properties of PPy–N and PA–N Composite Films

Figure 9 shows the dependence of current on applied potential for PPy–N and PA–N composite films. The currents increase linearly with the applied potential in both PPy–N and PA–N films, which means that ohmic conduction occurs predominantly in these composite films. The conductivity of PPy–N and PA–N films did not decrease with time in the atmospheric environment at room temperature. Therefore, it seems that the conduction in these composite films is not ionic but mainly electronic.

Figure 10 shows the temperature dependence of the surface conductivity for PPy–N and PA–N composite films. The conductivities of both PPy–N and PA–N films increase slightly with temperature and reach their maximum value at about 100°C and

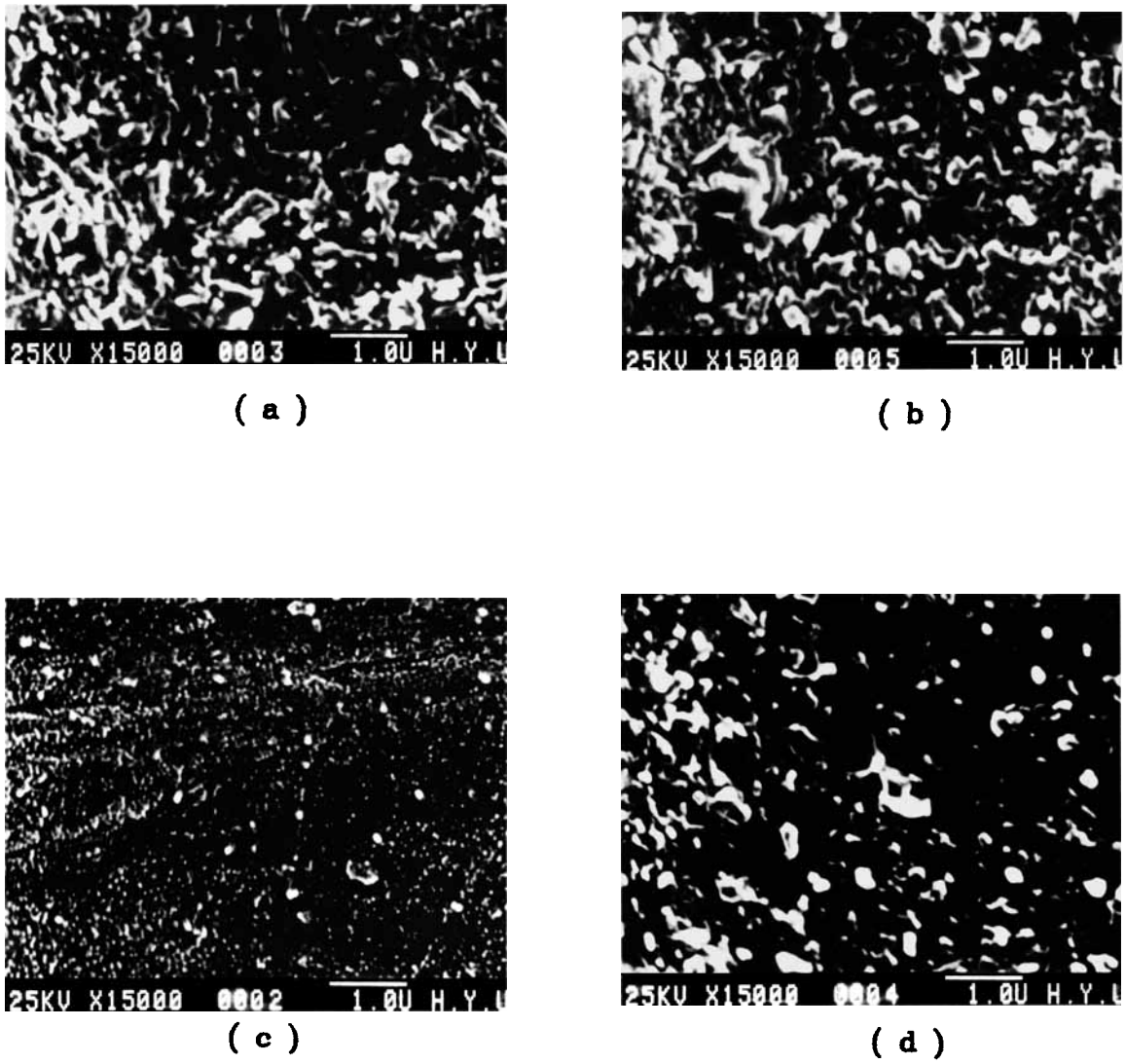

Figure 8 Scanning electron micrographs of PA–N composite film: $(NH_4)_2S_2O_8$ concentration 0.25*M*; polymerization time: 10 min; polymerization temp.: (a) 0°C; (b) 20°C; (c) 30°C; (d) 40°C.

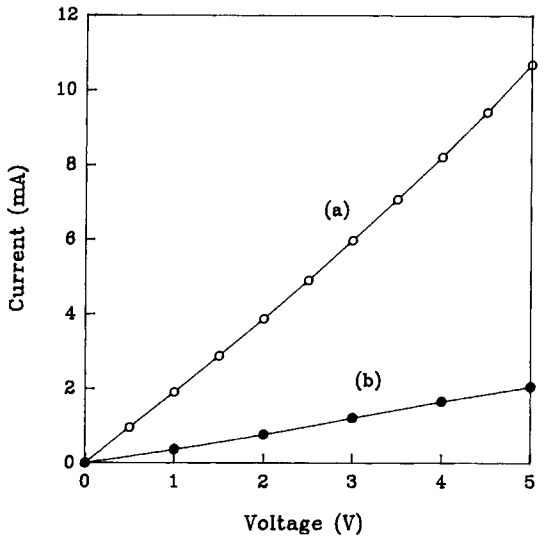

Figure 9 Dependence of current on applied potential for (a) PPy–N and (b) PA–N composite films. (a) polymerization temp.: 20°C; polymerization time: 2 h; $FeCl_3$ concentration: 2.0*M*. (b) Polymerization temp.: 20°C; polymerization time: 10 min; $(NH_4)_2S_2O_8$ concentration: 0.125*M*; HCl concentration: 1*M*.

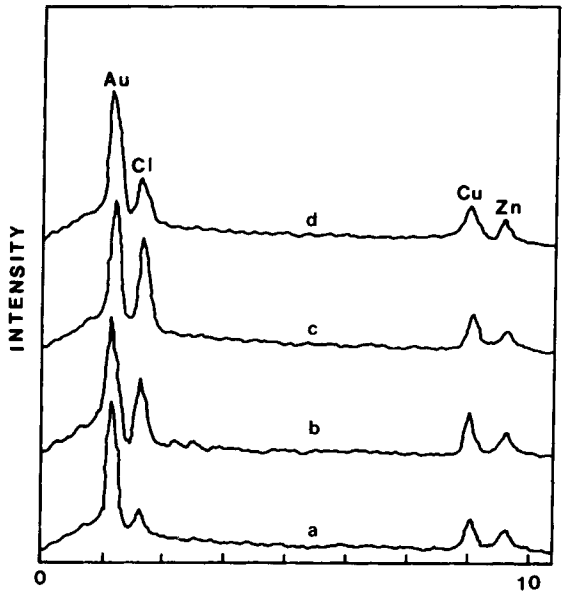

Figure 11 Graphical X-ray microanalysis data of PPy–N composite films: (a) conductivity, 2.85×10^{-4} (S/cm); (b) conductivity, 1.18×10^{-3} (S/cm); (c) conductivity, 2.38×10^{-3} (S/cm); (d) heat treatment of sample (c) at 140°C.

then tend to decrease. It seems that this decrease in conductivity is due to the dissociation of the dopant anion[18] such as Cl^-.

Figure 11 shows the graphical X-ray microanalysis data for the PPy–N composite film. The dopant chlorine ion of the PPy–N composite film plays an important role in the conduction process. The conductivity of the PPy–N composite tends to increase with Cl ion content. However, when the PPy–N composite film is annealed at 140°C for 30 min, the Cl ion content decreases considerably, as seen in Figure 11. This decrease of the Cl ion content is in accordance with the decrease of the conductivity in Figure 10.

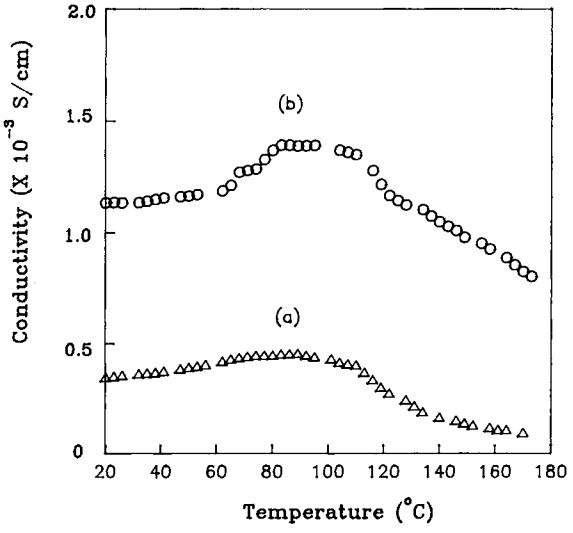

Figure 10 Temperature dependence of surface conductivity for (a) PPy–N and (b) PA–N composite films.

Mechanical Properties of the Composite Films

Figure 12 shows the effects of the polymerization time on the tensile strength and Young's moduli of PPy–N and PA–N composite films. The tensile strengths of both PPy–N and PA–N composite films decrease slightly with the polymerization time [Fig. 12(c) and (d)]. It seems that this behavior is caused by partial destruction of the crystalline region of nylon 6 as polypyrrole is polymerized in nylon 6 film, as seen in X-ray diffraction patterns (Fig. 2). The Young's moduli of these composite films tend to increase with the polymerization time [Fig. 12(a) and (b)]. It seems that these increments are caused by the reinforcement effect in the composites owing to the formation of the rigid polypyrrole or polyaniline in nylon 6 films. Therefore, it was found that PPy–N and PA–N composite films exhibited excellent mechanical properties.

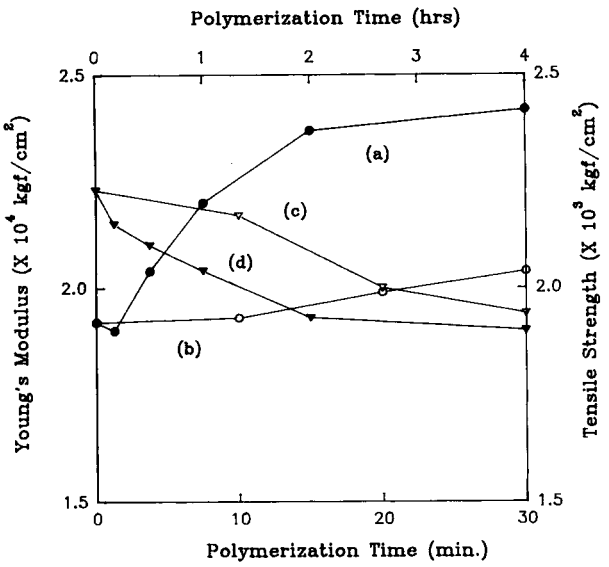

Figure 12 Effect of polymerization time on tensile strength and Young's modulus of PPy–N and PA–N composite films. Young's modulus: (a) PPy–N; (b) PA–N composite films. Tensile strength: (c) PPy–N; (d) PA–N composite films.

CONCLUSIONS

It was found that highly transparent and conducting PPy–N and PA–N composite films could be prepared by diffusion and chemical oxidative polymerization. The conductivity and transmittance of these composite films were affected by the preparative conditions, which might be due to the difference of their morphology. The mechanical properties of these composite films also depended on the polymerization conditions, which might be related to the change of crystal structure and reinforcement effect of polypyrrole or polyaniline in nylon 6 film. Further work is in progress to obtain more highly transparent and conducting composite films that are applicable to industry and to exploit practical application of these composite films.

This work was carried out under a research grant from the Korea Science and Engineering Foundation (9223-0006).

REFERENCES

1. K. L. Chopra, S. Major, and D. K. Pandya, *Thin Solid Films,* **102,** 1 (1983).
2. J. Y. W. Seto, *J. Appl. Phys.,* **46,** 5247 (1975).
3. D. Jousse, *Phys. Rev.* B, **31,** 5335 (1985).
4. I. Hamberg and C. G. Grangvist, *J. Appl. Phys.,* **60,** R123 (1986).
5. M. Kojima, H. Kato, A. Imai, and A. Yoshida, *J. Appl. Phys.,* **64,** 1902 (1988).
6. S. Nishikawa, *Thin Solid Films,* **135,** 219 (1986).
7. T. Ojio and S. Hiyata, *Polym. J.,* **18,** 95 (1986).
8. C. J. Li and Z. G. Song, *Syn. Met.,* **40,** 23 (1991).
9. N. F. Bakeev, *Macromol. Chem. (Suppl.),* **6,** 287 (1984).
10. L. H. Sperling, *Introduction to Physical Polymer Science,* Wiley, New York, 1986.
11. C. J. Durning, L. Rebenfeld, W. B. Russel, and H. D. Weigmann, *J. Polym. Sci. Polym. Phys. Ed.,* **24,** 1321 (1986).
12. J. Crank and G. S. Park, *Diffusion in Polymers,* Academic Press, New York, 1968.
13. J. Crank, *The Mathematics of Diffusion,* Clarendon Press, Oxford, 1975.
14. G. B. Street, T. C. Clake, M. Krounbi, K. Kanazawa, V. Lee, P. Pfluger, J. C. Scott, and G. Weiser, *Mol. Cryst. Liq. Cryst.,* **83,** 253 (1982).
15. M. Wan, *Syn. Met.,* **31,** 51 (1989).
16. M. Kuzmany and N. S. Sariciftic, *Syn. Met.,* **18,** 353 (1987).
17. A. P. Monkman, D. Bloor, G. C. Stevens, and J. C. H. Stevens, *J. Phys. D Appl. Phys.,* **20,** 1337 (1987).
18. M. Osagawa, K. Funahashi, T. Demura, T. Hagiware, and K. Iwata, *Syn. Met.,* **14,** 61 (1986).

Received April 5, 1993
Accepted August 9, 1993